

# Highly-Conductive Graphite Thermal Straps Used in Conjunction with Vibration Isolation Mounts for Cryocoolers

S.J. Nieczkoski and E.A. Myers

## ABSTRACT

Despite momentum balancing and active damping methods often utilized to mitigate vibration transmission from mechanically driven cryocoolers, sometimes it is still necessary to incorporate an external mechanical isolation mounting subsystem that will further attenuate coupling of mechanical disturbances into sensitive instruments or electro-optical systems. By incorporating a means for mechanical isolation of cryocooler compressors, a compromise is necessarily made in the elimination of straight-forward heat rejection through solid materials and hard-bolted interfaces. Since the performance of space-borne cryocoolers is highly sensitive to the thermal efficiency of heat rejection from the compressor, it is critical that a method for heat transport be devised without adversely impacting the relevant damping characteristics of the mechanical mounting system. Graphite fiber thermal straps (GFTS) provide an optimum combination of properties including high-thermal conductivity, low-mass, and low-stiffness for a thermal subsystem designed to be used in conjunction with a cryocooler compressor isolation mount. This paper discusses the challenging design parameters and resulting configuration of a GFTS-based heat rejection approach for dewar-mounted cryocoolers that are mechanically isolated from the heat rejection interface. Performance of the thermal subsystem and the interactive aspects with respect to the mechanical damping subsystem are presented.

## INTRODUCTION

The Soft X-Ray Spectrometer (SXS) on board JAXA's ASTRO-H Mission uses redundant pairs of two-stage Stirling cryocoolers, a Joule-Thomson cryocooler, 40-liters of superfluid helium, and a three-stage adiabatic demagnetization refrigerator to cool its microcalorimeter detectors to 50 mK.<sup>1</sup> During testing with the SXS Engineering Model, micro-vibration from the Stirling cryocoolers caused temperature fluctuation that adversely impacted detector performance at the 50 mK stage. The most deleterious vibration was in the 100-400 Hz band. Since the compressors dissipate heat that must be efficiently removed to keep them operating in an acceptable temperature range, simply eliminating the direct bolted interfaces between the compressors and the dewar vacuum shell was not a realistic option. Instead, a complete vibration isolation subsystem (VIS) incorporating both mechanical decoupling from and thermal attachment to the dewar vacuum shell was required to mitigate the detector thermal stability issue.



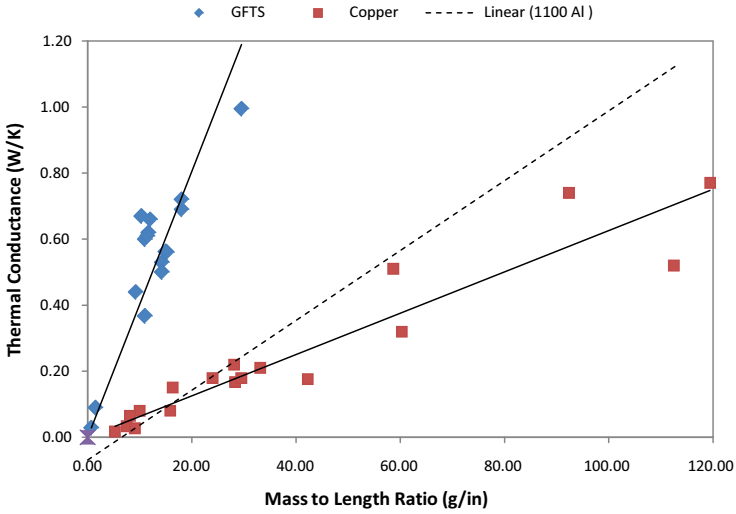


Figure 2. GFTS thermal conductance is far superior to metal straps at 300 K.

fittings, there is some efficiency loss. Achieving low-loss termination into the end fitting is one of the primary attributes of a quality thermal strap.

In the VIS configuration shown in Figure 1, there are seven individual GFTS units consisting of five unique designs. The strap interface areas and cross-sections are maximized within the available volume and attachment limitations on both ends. Figure 3 shows the five unique GFTS strap configurations.

Of these seven straps, the inner three straps conduct 55% of the total heat from the compressor due to the proximity to the heat rejection interface on the compressor flange and relatively short distance between interfacing ends. However, these three straps are also significantly stiffer than the other four straps due to shape and length. In designing the GFTS configurations to meet the thermal performance requirement, it was necessary to account for thermal resistance within the compressor case, the compressor mounting plate, dewar mounting plate, and across all bolted interfaces in the thermal path. Doing so resulted in a sum conductance for the thermal straps alone of nearly twice the requirement that was then reduced by the series of resistances in the thermal network. Given the relative maturity levels of both the compressor and vacuum shell designs, there was no allowance for additional thermal interface area at either the dewar or compressor locations. In order to attain more thermal strap attachment area and still utilize available packaging volume, the compressor and dewar interface plates that were designed to provide mechanical isolation were also configured to move heat away from the

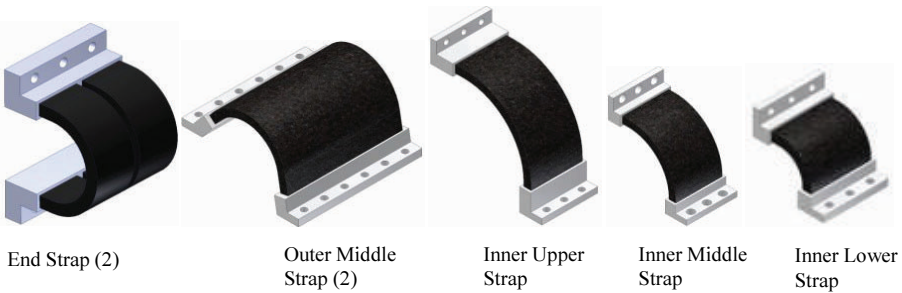
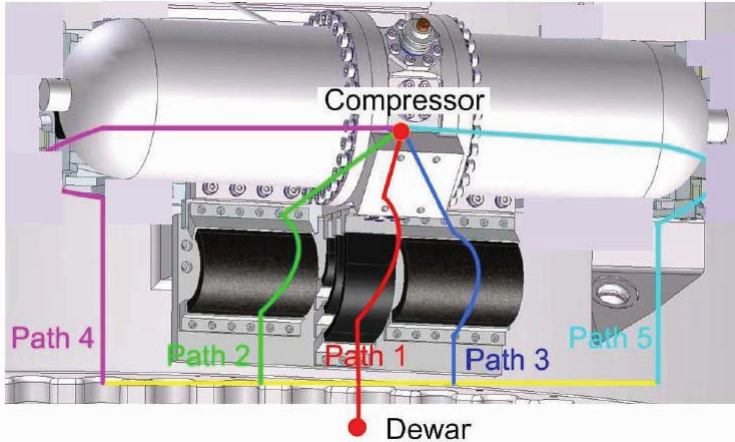


Figure 3. Five unique strap configurations that conform to allowable envelope.



**Figure 4.** Thermal paths from compressor case to dewar vacuum shell.

compressor flange and feet. Four of the seven straps are mounted from the VIS compressor interface plate. This plate is split into two separate sections and is bolted to the compressor center flange. The split arrangement is to facilitate integration, but it also results in somewhat asymmetric heat transfer.

### THERMAL NETWORK MODEL

As part of the design effort to establish the GFTS configurations, a thermal model of the integrated VIS was constructed to predict overall thermal conductance from the compressor case and flange to the dewar vacuum shell. All the heat transfer components of the subsystem were modeled using standard heat transfer equations, then the individual components were linked together to form a network model. Figure 4 depicts a representation of the thermal network used during the design and analysis effort.

The model also allowed for parametric studies on the performance dependencies of potential variables within the overall thermal/mechanical network. The simpler thermal network model was correlated with a more extensive finite-element thermal analysis that validated the model's predictive capability.

### INDIVIDUAL GFTS PERFORMANCE TESTING

While the thermal conductivity of the graphite fiber material approaches 1100 W/m K at room temperature, the GFTS manufacturing process is critical to realizing a significant level of efficiency with the raw material. TAI has been able to repeatedly demonstrate GFTS performance in excess of 90% of the theoretical maximum based upon the graphite material conductivity alone. Considering most thermal straps contain in excess of  $10^6$  individual fibers, this level of strap efficiency is compelling. Further, we have developed proprietary thermal performance models that have the predictive capability within 10% of measured performance for most strap configurations. As a standard measure to ensure performance and manufacturing quality control of GFTS units, each individual unit is thermal performance tested subsequent to fabrication and inspection and prior to delivery. If an issue with materials or construction were to occur, it will be revealed by lower than expected thermal conductance. All seven GFTS units fabricated and tested for the VIS were equal to or better than predictions. When added together, the set of GFTS units is expected to conduct 4.8 W/K including the contact resistances across the bolted interfaces at both ends. Table 1 contains the results of the modeled and tested thermal

**Table 1.** Individual GFTS Thermal Conductance Results

GFTS Unit	C (Test) (W/K)	C (predicted) (W/K)	Deviation (%)
SC Inner-Lower	0.645	0.572	+12.8
SC Inner-Middle	0.444	0.381	+16.5
SC Inner-Upper	0.356	0.339	+5.0
SC End 1	0.515	0.460	+12.0
SC End 2	0.526	0.460	+14.3
SC Outer 1	1.146	1.151	-0.3
SC Outer 2	1.148	1.151	-0.3

conductance for each of the GFTS units. The values in the table include the straps and the bolted interfaces in the stated conductance values.

Thermal strap stiffness is also a controlled performance parameter. In order to meet the momentum damping requirement for the VIS, the collective stiffness of the straps cannot exceed  $10^3$  N/mm in any axis. To determine stiffness, each of the GFTS units was characterized with test apparatus that is designed to measure the force and distance relationship of a strap independently in each of the three linear axes. Figure 5 shows a representative GFTS mounted in the stiffness measuring equipment.

To conduct a single axis measurement, a strap is mounted in the fixture with one end bolted to a stationary interface and the other end to a moving platform. Starting with the strap in its as-built (or null) position, the platform is moved in a controlled linear step to a new position. The force required to move and retain the strap in the new position is then measured; movement in other axes is constrained during each axial step and measurement.

The results from this testing provide the measured spring rate or stiffness of the strap in each axis. Figure 6 shows the stiffness testing results for each GFTS contained within the VIS engineering development unit (EDU). As expected, each strap has the most stiffness in the x-direction, defined by the direction of compressing the strap between terminals. Overall, the total stiffness of all straps in any one direction is less than 28 N/mm, or roughly 40 times lower than

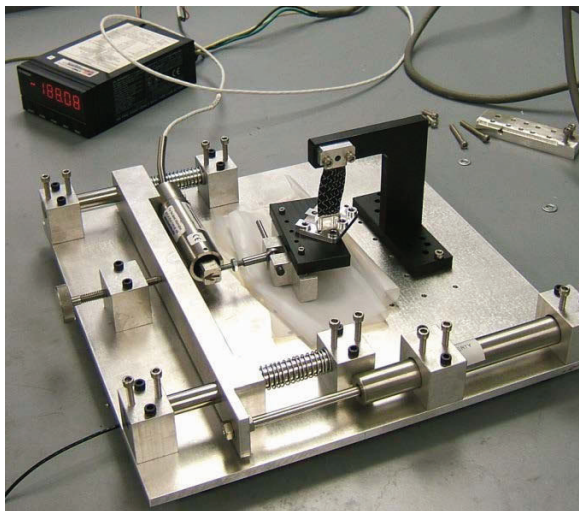


**Figure 5.** Thermal strap stiffness testing.

Unit	Stiffness (N/mm)			weight (g)
	X	Y	Z	
Inner-Lower	15.6	1.3	2.2	17.5
Inner-Middle	2.1	0.5	1.0	21.0
Inner-Upper	1.2	0.2	0.8	22.7
Outer-1	3.9	1.2	1.5	59.2
Outer-2	3.8	1.2	1.4	57.9
End-1	0.7	0.3	0.3	26.9
End-2	0.5	0.2	0.3	26.5

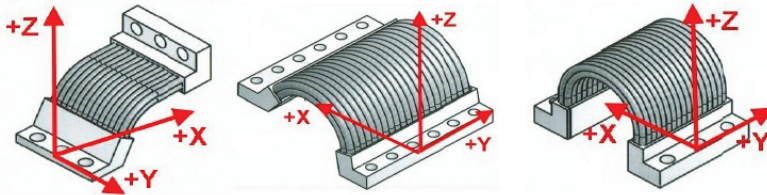


Figure 6. Individual GFTS stiffness measurement results.

the required level. The inner strap is the stiffest of the seven GFTS units because it has the shortest length and least amount of curvature.

**SUBSYSTEM THERMAL TEST**

The primary purpose of the sub-system level thermal test was to provide experimental data points to validate the predicted end-to-end thermal conductance within the VIS EDU and to provide data to correlate the model of the compressor-to-dewar thermal conductance network. Temperature sensor instrumentation location was established to determine the thermal resistance across each component and bolted interface between the heat dissipation source (compressor simulator) and the heat sink (dewar plate simulator).

The VIS EDU thermal test setup is shown by the photographs in Figure 7. The VIS EDU during this testing was comprised of the mounting plates for the compressor and on the dewar (upper and lower), the compressor simulator (heater block), dewar simulator (sink block), and the GFTS units. Thermocouples were embedded in all metal components to be within the heat flow path and consistent with relevant resistances contained in network model, especially across bolted interfaces. From many years of thermal test experience, TAI has found that attaching temperature sensors to the exterior of components rather than mounting them internally within the structure frequently introduces measurement error. While simpler to implement, surface mounting often moves the temperature measurement away from the significant heat flow path.

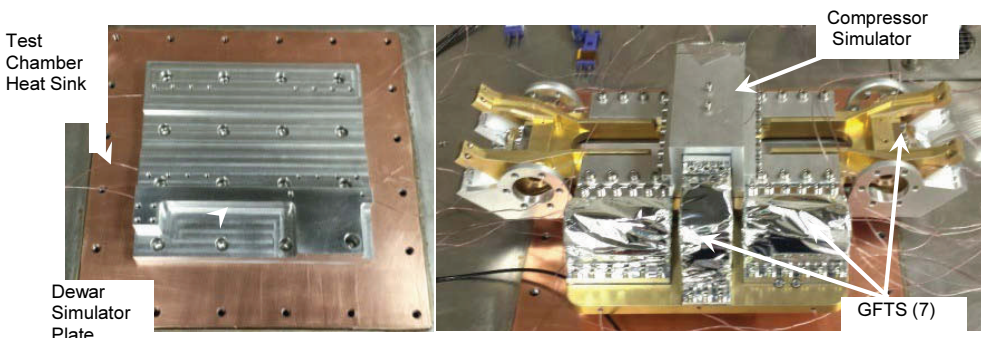


Figure 7. VIS EDU thermal test setup.

Table 2. VIS EDU thermal test results.

CHARACTERISTIC	REQUIREMENT	PREDICTED	MEASURED
Overall conductance (W/K)	≥ 2.5 (goal)	2.4	2.1
Left-right Temp gradient	Minimize	None	< 2.0
Front-back Temp gradient	< 10 K	< 10 K	< 6.5 K

A test sequence consisted of applying power to the heater contained within the compressor simulator after a sufficient vacuum level had been achieved, then monitoring temperatures until equilibrium had been reached; equilibrium was defined by all temperatures being stable within 0.1°C over a 30 minute period. A total of 28 thermocouples were monitored during each test sequence including those within the EDU structure and attached to the vacuum shell to determine the ambient thermal condition.

Heater voltage, heater current, and thermocouples were monitored, read, and recorded by a computerized data acquisition program. Raw data were written to data files for reduction and specific calculations that were later used to determine both overall and local thermal conductance values within the thermal network.

**SUBSYSTEM THERMAL TEST RESULTS ANALYSIS**

Two series of tests were conducted at power levels of 63 W and 40 W, respectively. The data from the nominal 63W dissipation level test were used to calculate heat flows, overall and individual conductance values through solid materials, and bolted interface resistances. Data from the 40 W test condition were used to determine parasitic heat leak away from the subsystem and to validate and correlate the thermal network model.

By correlating the measured temperature drop across each GFTS unit in the subsystem test and the measured conductance values obtained from individually testing each of the GFTS units, the heat flow through each major path within the network model could be calculated from the temperature sensor data. Once the heat flow levels in the primary paths were determined, calculating interface resistances and temperature symmetries was relatively straightforward.

Overall the thermal conductance from the center of the compressor simulator to the dewar simulator was roughly 15% lower than predicted (see Table 2). Initial analysis using the recorded data and the thermal network model indicates that the thermal conductance values across most bolted interfaces were less than the modeled values. This could be the result of limited number and size of fasteners available to achieve efficient contact force at these locations. Currently, methods to improve metal-to-metal interface conductance, possible plate material changes, and the addition of additional GFTS are being evaluated as a means to increase overall thermal performance.

Despite the GFTS arrangement that is biased toward one side of the compressor, testing showed that temperature symmetry was within required limits. Temperatures in the dewar simulator were fairly uniform, indicating good heat flow distribution. In the compressor simulator, the right-to-left temperatures were evenly distributed, while temperatures on the compressor back side (opposite the GFTS) were less than 6.5 K higher than the front side. Since the configuration constraints mandated that the GFTS be located only on one side of the compressor, there was concern that temperature asymmetry of > 10 K could exist that might cause degradation in compressor performance. Modeling and testing have shown that this will not be an issue in this thermal management system.

**CONCLUSION**

GFTS technology enables a completely passive thermal management solution in applications that require a high-level of efficiency in moving heat, such as the space-flight cryocooler VIS discussed here. With highly restrictive requirements resulting from a mature